Principles of Adaptive Space-Time-Polarization Cancellation of Broadband Interference

Ronald L. Fante, *The MITRE Corporation, Bedford, Massachusetts 01730-1420*

Abstract

In this paper, we discuss and analyze the method of operation of a space-time-polarization adaptive array. We demonstrate by simulation that an array of N dual-polarized antennas can cancel up to 2N-1 broadband interferers, while still allowing detection of desired signals over a significant portion of a half-space.

I. Introduction

There has been a great deal of research [1-15] on the ability of adaptive space-time (ST) antennas to cancel interference in an antenna array, but little has been done on the value of adding polarization, thus, creating a space-time polarization (STP) canceller. In the STP canceller, we have N dual-polarized antennas, with an adaptive finite impulse (FIR) filter behind each antenna port, leading to (2N-1) degrees of freedom as shown in Figure 1. The delays T in Figure 1 are equal to intersample period, and are used to compensate for broadband dispersive effects. Thus, the space-time-polarization array can achieve 2N-1 degrees of freedom using only one half the area required by a conventional non-polarimetric array. This is an important consideration when cancellers must be mounted on airborne platforms where the available area is limited, or for hand-held receivers.

Unfortunately, many people do not understand how the polarization dimension works or do not believe that using N dual-polarized elements really creates (2N-1) degrees of freedom, and consequently, the potential ability to cancel 2N-1 broadband interferers. The purpose of this paper is to explore this issue. In order to provide insight into polarization cancellation, we will first consider the simplest case of a single dual-polarized element, and demonstrate that this can cancel an interferer with an arbitrary polarization state without necessarily cancelling desired signals, unless the desired signal is at the same angular location as the interferer and has the same polarization state. We then generalize the treatment to the case of an array consisting of N dual-polarized elements, and demonstrate that, although the array cannot perfectly cancel 2N-1 strong, broadband interferers it does a reasonable job. Although our discussions will be valid for any case, our applications will be primarily to the global positioning system (GPS) [16-17].

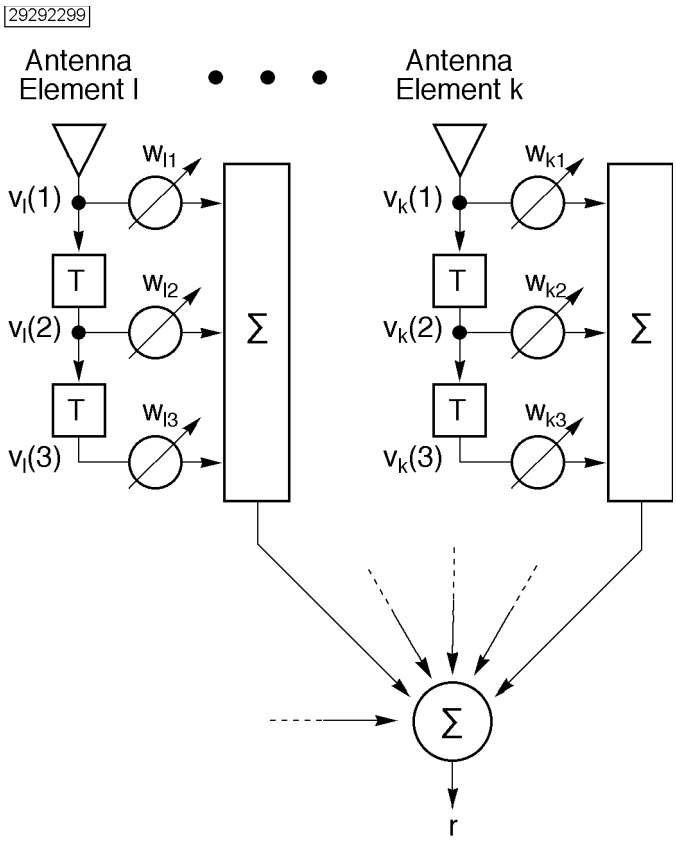

Figure 1. Adaptive Space-Time Polarization Array

II. Single-Element Limit

Let us first discuss the simplest possible space-time-polarization canceller. This consists of a single dual-polarized element in which interference is cancelled by weighting the output v_2 of port 2 by a constant w and subtracting it from the output v_1, of port 1. Ports 1 and 2 may be either orthogonal, linearly polarized ports, or right and left circularly polarized ports, obtained by combining the two orthogonal linearly polarized ports. The weight w can be determined by minimizing the expected residual power $E\left(|r|^2\right)$, where $r = v_1 - w\,v_2$. If this is done, we find

$$w = \frac{E\left(v_1 v_2^*\right)}{E\left(|v_2|^2\right)} \tag{1}$$

so that the expected output power is

$$E\left(|r|^2\right) = E\left(|v_1|^2\right) - \frac{\left|E\left(v_1 v_2^*\right)\right|^2}{E\left(|v_2|^2\right)}. \qquad (2)$$

We now evaluate Equation (2) for a single interferer at angular location (θ,ϕ) in the spherical coordinate system, shown in Figure 2. Suppose $\mathbf{J}(f) = J(f)\left(\alpha_\theta\hat{\theta} + \alpha_\phi\hat{\phi}\right)$ is the Fourier transform

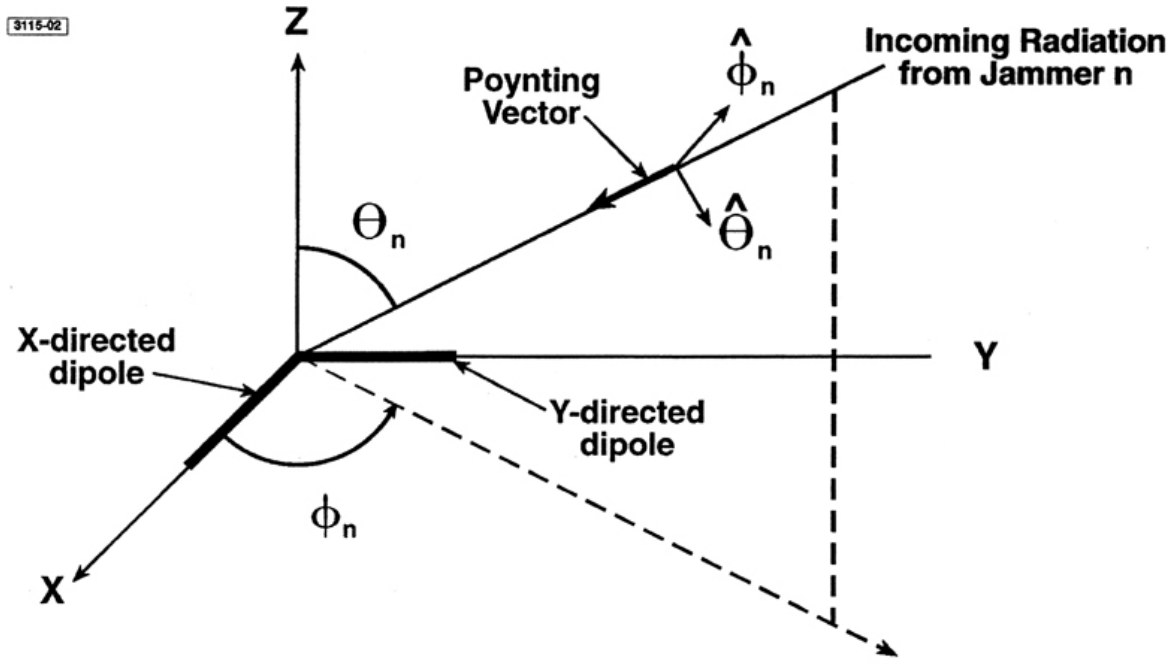

Figure 2. Jammer *n* Radiation Incident on Dual-Polarized Antenna

of the interferer electric field vector and $g_p(f,\theta,\phi) = g_{p\theta}(f,\theta,\phi)\hat{\theta} + g_{p\phi}(f,\theta,\phi)\hat{\phi}$ is the Fourier transform of the vector voltage-gain of antenna port p, where $\hat{\theta},\hat{\phi}$ are unit vectors along (θ,ϕ) in a spherical coordinate system centered on the antenna. Analytical expressions for g_θ, g_ϕ for a microstrip patch may be found in Reference 18. The unit vector $\boldsymbol{\alpha} = \alpha_\theta\hat{\theta} + \alpha_\phi\hat{\phi}$ defines the polarization state of the jammer. For example, for a circularly-polarized jammer $\alpha_\theta = 1/\sqrt{2}$ and $\alpha_\phi = i/\sqrt{2}$. Using these definitions, we then see that if there is a brick-wall filter of bandwidth B in each channel, the voltage produced by the jammer on port p is

$$v_p(t) = K \int_{-B/2}^{B/2} df\ \mathbf{J}(f) \cdot \mathbf{g}_p(f,\theta,\phi)\, e^{i2\pi ft} + s_p(t) + x_p(t)\,, \tag{3}$$

where t = time, f = frequency, p = 1, 2, K_o is a constant of proportionality, the dot denotes an inner product, $x_p(t)$ is the noise on port p and $s_p(t)$ is the desired signal, which is assumed to lie below the noise floor. For the moment, the signal will be ignored.

By using Equation (3), it is readily shown that if the jammer voltage is a statistically-stationary random process, then

$$E\left(v_p v_q^*\right) = |K_o|^2 \int_{-B/2}^{B/2} df\ \Phi(f)\left(\boldsymbol{\alpha}\cdot\mathbf{g}_p\right)\left(\boldsymbol{\alpha}^*\cdot\mathbf{g}_q^*\right) + \sigma^2\delta_{pq}\,, \tag{4}$$

where the arguments (f,θ,ϕ) have been suppressed in $g_p(f,\theta,\phi)$, $\Phi(f)$ is the jammer power spectral density, σ^2 is the noise power, and δ_{pq} is the Kronecker delta.

For a narrowband interferer $(B \to 0)$, Equation (4) reduces to

$$E\left(v_p v_q^*\right) = P_J\left(\boldsymbol{\alpha}\cdot\mathbf{g}_p(0)\right)\left(\boldsymbol{\alpha}^*\cdot\mathbf{g}_p^*(0)\right) + \sigma^2\delta_{pq}\,, \tag{5}$$

where P_J is the jammer power that would be received by an isotropic antenna with a receive polarization matched to the jammer polarization state. Also, $\mathbf{g}_p(0) = \mathbf{g}_p(0,\theta,\phi)$ denotes the midband vector voltage gain. By using Equation (5) in Equation (1) we readily see that, in the narrowband limit and when the received jammer power greatly exceeds the channel noise, the weight applied is approximately,

$$w = \frac{\boldsymbol{\alpha}\cdot\mathbf{g}_1(0,\theta,\phi)}{\boldsymbol{\alpha}\cdot\mathbf{g}_2(0,\theta,\phi)}. \tag{6}$$

Equations (5) and (6) are valid only in the narrowband $(B \to 0)$ limit. For wideband jammers, we must consider the effects of the frequency dispersion of the two channels. In order to include dispersion, we approximate the dispersive voltage gain of the two antenna ports as (p = 1,2)

$$\mathbf{g}_p(f,\theta,\phi) = \mathbf{g}_p(0,\theta,\phi)\left(1 + a_p\frac{f}{B}\right)\exp\left(ib_p\frac{f}{B}\right) \tag{7}$$

for frequency $|f| \le B/2$. Any receiver dispersion is included in Equation (7). That is, we assume that the bandwidth B is such that the amplitude and phase variations relative to band center can

be approximated by the first two terms in their Taylor series expansions. The quantity a_p is the total amplitude deviation across the bandwidth B and b_p is the total phase variation.

Now, if we assume the jammer power spectrum is white, substitute Equation (7) into Equation (4) and then use Equation (4) in Equation (2), we obtain after considerable manipulation

$$E\left(|r|^2\right) = \sigma^2\left[1 + \frac{JNR_1}{1+JNR_2} + \frac{JNR_1}{12}\left(\Delta a^2 + \Delta b^2\right)\right], \tag{8}$$

where $\Delta a = a_1 - a_2$, $\Delta b = b_1 - b_2$ and JNR_p is the unadapted jammer-to-noise ratio in channel p at midband, defined as

$$JNR_p = \frac{P_J\left|\boldsymbol{\alpha}\cdot\mathbf{g}_p(0,\theta,\phi)\right|^2}{\sigma^2}. \tag{9}$$

The last term on the right hand side of Equation (8) shows the effect of mismatch between Channels 1 and 2, and indicates how closely the channels must be matched so that the residue after adaptation is not significantly greater than σ^2. In particular, we require that

$$\Delta a^2 + \Delta b^2 < \frac{12}{JNR_1}. \tag{10}$$

When Equation (10) is satisfied, it is evident from Equation (8) that the residue after adaptation will be of order σ^2, unless the jammer/antenna configuration is such that $JNR_1 >> JNR_2$, or equivalently, $\left|\boldsymbol{\alpha}\cdot\mathbf{g}_1(0,\theta,\phi)\right| >> \left|\boldsymbol{\alpha}\cdot\mathbf{g}_2(0,\theta,\phi)\right|$. Thus, we have demonstrated that it is possible to cancel a broadband jammer without using spatially-separated antennas or temporal degrees of freedom.

It is also important to calculate the response at angles other than the angular location of the jammer, because we need to know whether desired incoming signals can be detected (i.e., we need to ensure that the null doesn't extent over all angles). Therefore, let us compute the response to a signal with a polarization vector $\boldsymbol{\alpha}'$ at an angular location (θ',ϕ') that is different from the jammer location. The response is

$$\left|r(\theta',\phi')\right|^2 = \left|v_1(\theta',\phi') - w\,v_2(\theta',\phi')\right|^2. \tag{11}$$

We now consider the narrowband limit and ignore noise. In this case, $v_p = A\boldsymbol{\alpha}'\cdot\mathbf{g}_p(0,\theta',\phi')$, for p = 1,2, where A is a constant that is proportional to the signal strength. Then, if we use this expression for v_p, along with Equation (6), in Equation (11), we find

$$\left|r(\theta',\phi')\right|^2 = \left|A\right|^2 \left|\boldsymbol{\alpha}'\cdot\mathbf{g}_1(0,\theta',\phi') - \frac{\boldsymbol{\alpha}\cdot\mathbf{g}_1(0,\theta,\phi)}{\boldsymbol{\alpha}\cdot\mathbf{g}_2(0,\theta,\phi)}\boldsymbol{\alpha}'\cdot\mathbf{g}_2(0,\theta',\phi')\right|^2. \qquad (12)$$

From Equation (12), we see that if $\boldsymbol{\alpha}' = \boldsymbol{\alpha}$ and $\theta' = \theta,\ \phi' = \phi$ the response is zero (i.e., a pattern null), but that a desired signal incoming at the same angular location $(\theta' = \theta,\ \phi' = \phi)$ as the jammer, but with a different polarization state $(\boldsymbol{\alpha}' \neq \boldsymbol{\alpha})$ is not cancelled completely. Furthermore, desired signals with the same polarization state $(\boldsymbol{\alpha}' = \boldsymbol{\alpha})$ but different locations $(\theta' \neq \theta,\ \phi' \neq \phi)$ are also not cancelled. Thus, only signals at the same location and polarization state as the jammer are nulled (down to the noise floor). However, signals at the same location, but with a different polarization state than the jammer are not completely nulled, and may be detectable depending on their strength. Of course, for targets at other angles $(\theta' \neq \theta,\ \phi' \neq \phi)$ and polarization states $(\boldsymbol{\alpha}' \neq \boldsymbol{\alpha})$ there is clearly no nulling.

III. General Case

Now let us discuss the general space-time polarization array shown in Figure 1, where there are N dual-polarized antennas, each with a K tap adaptive FIR filter*. Let us define a weight vector

$$\mathbf{w}^T = \left[w_{11}(1)...w_{11}(K)w_{12}(1)...w_{N2}(1)...w_{N2}(K)\right], \qquad (13)$$

where $w_{np}(k)$ is the weight applied to time tap k, port p (p = 1, 2) of antenna element n. Then, the output of the array can be written as

$$y = \mathbf{w}^T\mathbf{x}, \qquad (14)$$

where

$$\mathbf{x}^T = \left[x_{11}(1)...x_{11}(K)...x_{N2}(1)...x_{N2}(K)\right] \qquad (15)$$

with $x_{np}(k)$ equal to the voltage at time tap k of port p of antenna element n. The question we now answer is: "How should we compute the weight vector to be applied? There are many possible algorithms. In Section 2, we employed the simplest of all interference cancellation algorithms: we simply minimized the output power of the array, without placing any constraints

---

* As discussed in Reference 19, the purpose of the time taps is to compensate for dispersive effects, such as interference multipath and also to allow for cancellation of narrowband interferers (i.e., frequency nulls in addition to spatial nulls).

on the pattern gain in the direction of a desired signal (e.g., a GPS satellite). Because the desired signal is well below the noise floor (before processing) this approach is acceptable, but we can never be sure a priori what gain will be present in the direction of the desired incoming signal. Thus, one considers constrained algorithms. Below, we summarize a few, including the generalization of the simple "power minimization" algorithm. In Reference 19, we discuss and quantitatively compare the performance of these and multiple other potential algorithms.

a. Power Minimization

Let us first generalize the simple power minimization algorithm. Suppose the weight on the center tap of antenna element 1 is constrained to equal unity, and all other weights are left flexible. This constraint can be written as $w^T s_o = 1$ where $s_o^T = [0\,0 \ldots 1\,0\,0 \ldots 0]$ and the unity element in s_o^T occurs at (K + 1)/2, assuming K is odd. Because the desired signal is well below the noise floor, the output $y = w^T v$ of the array is primarily interference. Consequently, the interference power is

$$\begin{aligned} P_I &= E\left[y^* y\right] \\ &= w^H E\left(v^* v^T\right) w \ . \end{aligned} \tag{16}$$

If we now minimize the interference power P_I, subject to the constraint $w^T s_o = 1$, then using Lagrange multipliers, we find

$$w = \mu R^{-1} s_o \, , \tag{17}$$

where μ is a normalization constant and

$$R = E\left(v^* v^T\right) . \tag{18}$$

Specific expressions for the components of the covariance matrix R will be presented later.

b. Minimum Mean Square Error

In this approach, we minimize the mean square error between the desired signal $s_d(t, \theta, \phi)$ that would be received by an antenna (matched to the signal polarization) from a satellite at a specified angular location (θ, ϕ) and the output $y = w^T v$ of the adaptive array. That is, we minimize

$$\varepsilon = E\left[\left| s_d - w^T v \right|^2 \right], \tag{19}$$

where v is defined by Equation (15) and w is defined in Equation (13). We recall that

$$v_{np}(k) = z_{np}(k) + s_{np}(k), \tag{20}$$

where $z_{np}(k)$ is the interference plus noise and $s_{np}(k)$ is the signal that appears at time tap k, on port p of antenna element n. Note that z_{np} and s_{np} are statistically independent, so that $E\left(s_{np} z_{np}^{*}\right) = 0$.

If we use Equation (20) in Equation (19) then minimize E with respect to w we find

$$w = R^{-1} h, \tag{21}$$

where R is defined in Equation (18),

$$h = E\left(S^{*} s_d\right), \tag{22}$$

$$S^{T} = \left[s_{11}(1) \ldots s_{11}(K) \ldots s_{N2}(1) \ldots s_{N2}(K)\right]. \tag{23}$$

Note that, because GPS satellites usually transmit psuedorandom codes, s(t) is a random quantity, so the expectation is required in Equation (22). For deterministic signals, Equation (21) reduces to the result in Reference 10.

The one problem with the above approach is that a different weight vector is required for each GPS satellite (i.e., for each (θ, ϕ) specified). Thus, if Q satellites are in view, we require Q adaptive filters, and this makes the process computationally intensive. We can achieve a suboptimum result using a single weight vector by considering the next approach.

c. Minimum Mean Square Error Averaged Over Hemisphere

In this approach, we minimize the mean square error averaged over the upper hemisphere (or some portion thereof), as given by

$$\varepsilon' = \frac{1}{2\pi} \iint d\Omega \, E\left[\left| s_d(\theta, \phi) - w^{T} v \right|^{2}\right], \tag{24}$$

where $d\Omega = \sin\theta \, d\theta \, d\phi$. In this case, we find

$$w = R^{-1} h_o, \tag{25}$$

where

$$h_o = \frac{1}{2\pi}\iint d\Omega\, E\left[S^* s_d\right]. \tag{26}$$

In practice, it has been found that, while the solution in Equation (21) gives significantly better output signal to noise ratios after adaptation than does power minimization, the solution in Equation (25) gives only marginally better performance than power minimization.

IV. Covariance Components

In this section, we generalize the result in Equation (4) to calculate the covariance component $E\left[v_{np}(t)v^*_{mq}(t+\tau)\right]$. Let us define $\mathbf{g}_{np}(f,\theta,\phi)$ as the vector voltage gain of element n when port p is excited. Also, define $H_{np}(f)$ as the frequency response of this channel and G(f) as the frequency response of the front-end filter used on all channels. Then if there are N_J interferers with polarization states $\boldsymbol{\alpha}_j$ located at angular positions (θ_j,ϕ_j), the voltage received on port p of element n

$$v_{np}(t) = K_o \sum_{j=1}^{N_J} \int_{-\infty}^{\infty} df \boldsymbol{\alpha}_j \cdot \mathbf{g}_{np}\left(f,\theta_j,\phi_j\right) J_j(f) H_{np}(f) G(t) \cdot \exp(i2\pi ft) + x_{np}(t), \tag{27}$$

where $x_{np}(t)$ is the noise voltage on port p of element n. Because the desired signal is generally well-below the noise floor, it is not included in Equation (27). If all interferers are statistically independent and statistically stationary, then the component

$$R_{npmq}(\tau) = E\left[v_{np}(t)v^*_{mq}(t+\tau)\right]$$

of the covariance matrix R is

$$R_{npmq}(\tau) = \sum_{j=1}^{N_J} \int_{-\infty}^{\infty} df\, \boldsymbol{\alpha}_j \cdot \mathbf{g}_{np}\left(\theta_j,\phi_j\right)\boldsymbol{\alpha}^*_j \cdot \mathbf{g}^*_{mq}\left(\theta_j,\phi_j\right)\Phi_j \cdot |G|^2 H_{np}H^*_{mq}e^{i2\pi f\tau} + \sigma^2\rho(\tau)\delta_{nm}\delta_{pq}\ , \tag{28}$$

where the constant K_o has been omitted, $\Phi_j(f) = E\left[\left|J_j(f)\right|^2\right]$ is the power spectral density of interferer j, the frequency variable f has been suppressed in g, G, H, $\rho(\tau)$ is the normalized

autocorrelation function of the noise, σ^2 is the noise power and δ is the Kronecker delta. Note that the last term in Equation (28) is valid if both ports on each element are linearly-polarized or circularly polarized, but not for arbitrary elliptical polarization, because then the noise in two different ports of the same element is partially correlated.

It is also possible to include mutual coupling in Equation (28) by using the antenna scattering matrix. However, the details are cumbersome, and will be omitted here, although some of our later results will include mutual coupling effects.

V. Numerical Evaluations of Effectiveness

In this section, we evaluate the effectiveness of a planar array of dual-polarized elements. The first measure we will consider is the interference-plus-noise-to-noise ratio after adaptation, as given by

$$\mathrm{INR} = \frac{\mathbf{w}^H \mathbf{R} \mathbf{w}}{\mathbf{w}^H \mathbf{R}_N \mathbf{w}}, \tag{29}$$

where $\mathbf{w}^H$ is the conjugate transpose of w, $\mathbf{R}_N$ is the noise component of R. A second measure is the signal-to-interference-plus-noise ratio after adaptation, as given by

$$\mathrm{SINR} = \frac{\mathbf{w}^H \mathbf{R}_{SS} \mathbf{w}}{\mathbf{w}^H \mathbf{R} \mathbf{w}}, \tag{30}$$

where $\mathbf{R}_{SS} = \mathrm{E}\left(\mathbf{S}^* \mathbf{S}^T\right)$, and the vector $\mathbf{S}(\theta, \phi)$ is given by Equation (23). For all results to follow, we will assume that the weight vector is calculated using simple "power minimization" (see Equation (17)) and also perfect channel match (i.e., $H_{np} = 1$ in Equation (28)), so that the calculations represent a "best case" performance. Because the channel match is assumed perfect, we will not require adaptive time taps (unless the bandwidth is very large), so most of the results to follow will assume K = 1 in Equations (13), (15), etc.

Let us first evaluate the performance of a single dual-polarized antenna. We choose a square microstrip patch that lies in the z = 0 plane in Figure 2 with both ports 1 and 2 linearly polarized in the x and y directions, respectively. In Figure 3, we show the interference-plus-noise to noise ratio when there are up to three linearly (with randomly-oriented polarization vector) or circularly-polarized, broadband interferers (B = 24 MHz) randomly located in azimuth in an elevation band 0° to 20° above the horizon with each interferer producing an interference-to-noise ratio of 40 dB on each antenna element. Each point in Figure 3 is the average of 200 interferer locations and polarization direction (for the case of the linearly-polarized interferers). Mutual coupling between the x and y antenna ports is quite small (as verified by measurement)

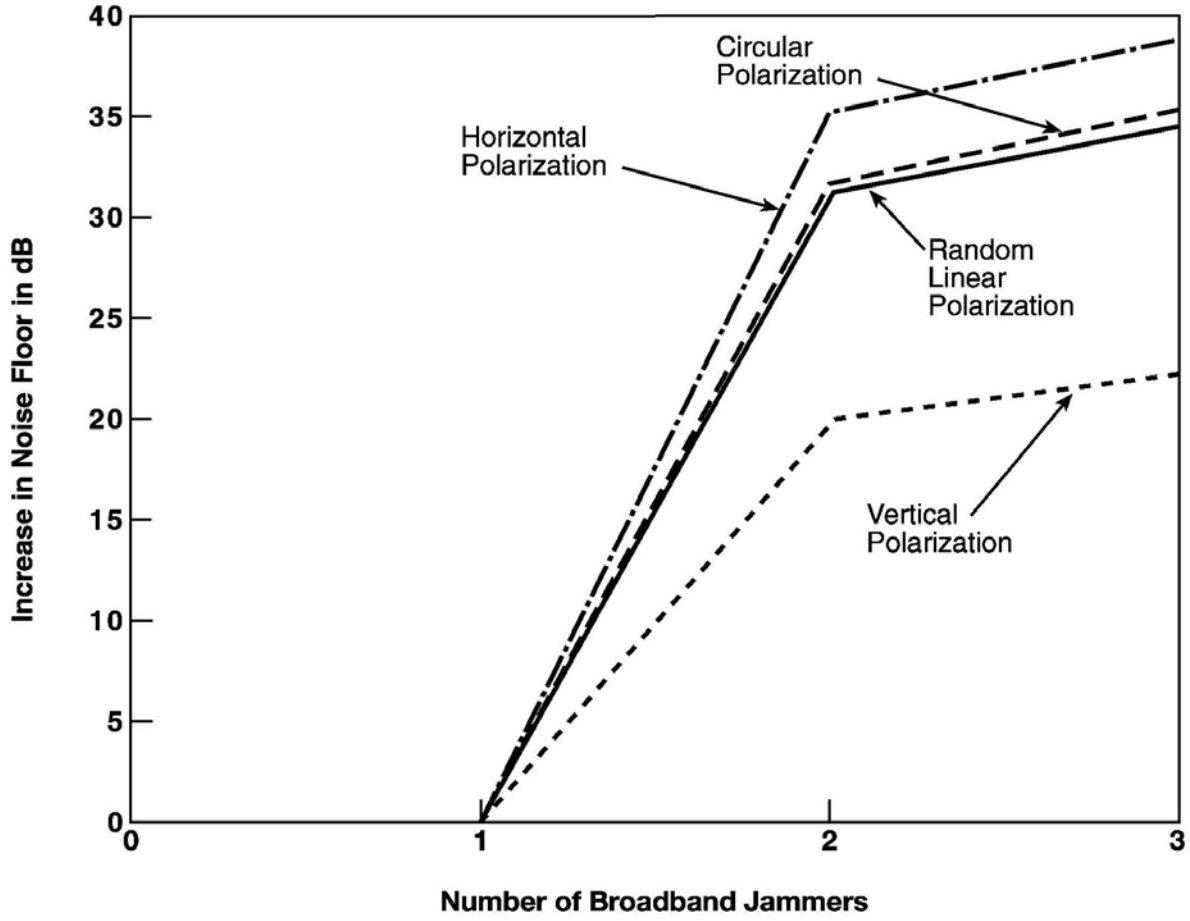

Figure 3. Performance of One Dual-Polarized Antenna

and has been ignored. From Figure 3 it is evident that the polarization canceller works very well in cancelling a single broadband interferer, but fails for two or more randomly-located interferers, as expected.

Of course, as mentioned earlier, just cancelling the interference is not sufficient. We also need to be able to see desired signals. In order to study this problem, we consider a typical GPS application. We wish to determine the fraction of the sky (upper hemisphere) where a GPS satellite signal will exceed a specified threshold in the presence of an interferer. Suppose an overhead satellite radiates a power such that a power P_r = -157.2 dBW is received by an isotropic antenna in the absence of any interference. Then this satellite will produce a carrier-to-noise ratio in a microstrip patch with a 3 dB gain G at zenith, a noise figure F = 4 dB and a loss L = 2 dB of

$$\frac{C}{N_o} = P_r + G - 10\log_{10}(kT_o) - F - L \quad \text{dB} - \text{Hz}$$

$$= 43.8 \text{ dB-Hz}, \tag{31}$$

where k = Boltzmann's constant and T_o = 290°K. For GPS systems, lock is lost when interference causes the carrier-to-noise ratio (C/N_o) to fall below specified thresholds. For conventional GPS systems that track only the GPS code (called State 3) the threshold is 16.5 dB-Hz if the GPS receiver is mounted on a quasi-static platform and 23 dB-Hz if the receiver is mounted on a dynamic platform, such as a high-performance aircraft. There are also high-precision GPS systems that actually track the carrier phase (called State 5). These lose lock if C/N_o falls below 18.5 dB-Hz for quasi-static platforms and 28 dB-Hz for dynamic platforms. We will now present some results for GPS satellite availability in terms of C/N_o.

We consider a single broadband (24 MHz) interferer located randomly in azimuth (0° to 360°) and elevation (0° to 20°), and then use Monte Carlo techniques to find the probability that a GPS satellite located randomly in the upper hemisphere (minus a 10° elevation mask at the horizon) will produce a signal that exceeds a specified carrier-to-noise ratio in a single dual-polarized antenna. The results of this simulation are shown in Figure 4. The ordinate is the probability (which we define as satellite availability) of exceeding the value of C/N_o on the abscissa. From Figure 4, we see that even in the presence of a fairly-strong, broadband interferer (J/N = 40 dB), there is a 0.95 probability that we will be able to maintain dynamic State 5 lock on any GPS satellite in the upper hemisphere (minus a 10° elevation mask at the horizon). This is indeed excellent performance, and demonstrates only a small loss in system performance relative to the interference-free case (for the interference-free case the satellite availability in unity for C/N_o = 28 dB-Hz).

Next consider two dual-polarized square, microstrip antennas lying with the z = 0 plane, with a spacing of one-half wavelength between the phase centers of the two antennas. This array now has three adaptive degrees of freedom. Broadband interferers (24 MHz) are now placed randomly in azimuth in an elevation band of 0° to 20° above the horizon. The interferers may be either circularly polarized or linearly polarized with a random polarization vector ($\hat{\theta}\cos\psi + \hat{\phi}\sin\psi$, where ψ = random $(0,2\pi)$). The performance of this array is shown in Figure 5. Each point in that figure is the average of 200 jammer realizations. As expected*, up to three* broadband interferers can be cancelled down to and below the noise floor, but four or more broadband interferers overwhelm the array.

---

* We also studied the case of one broadband noise jammer with dual independent, orthogonal polarizations plus a second randomly located linear or circularly polarized jammer. This combination is equivalent to three jammers, and was cancelled by the pair of dual polarized antennas. However, two jammers, each with independent orthogonal polarizations are equivalent to four jammers and were not cancelled.

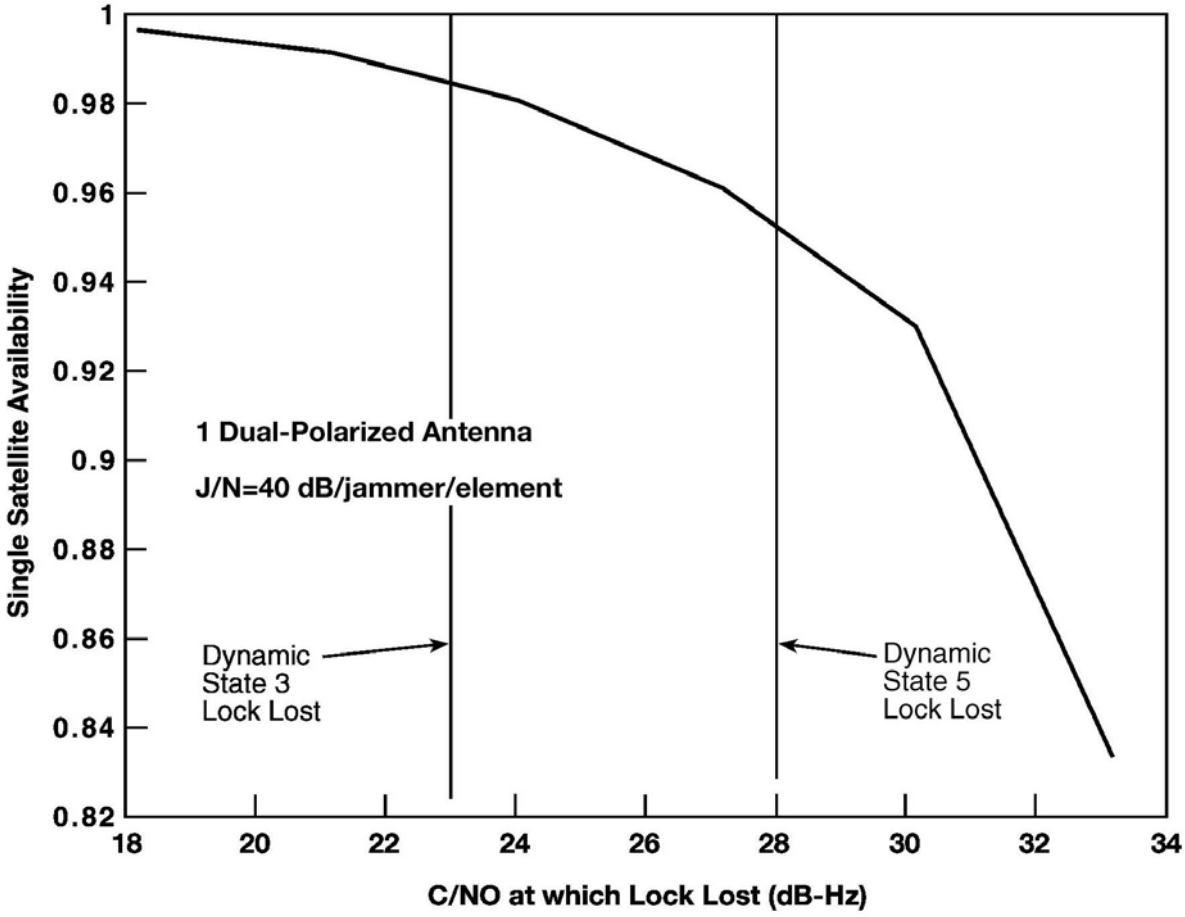

Figure 4. Availability in the Presence of One Broadband Jammer

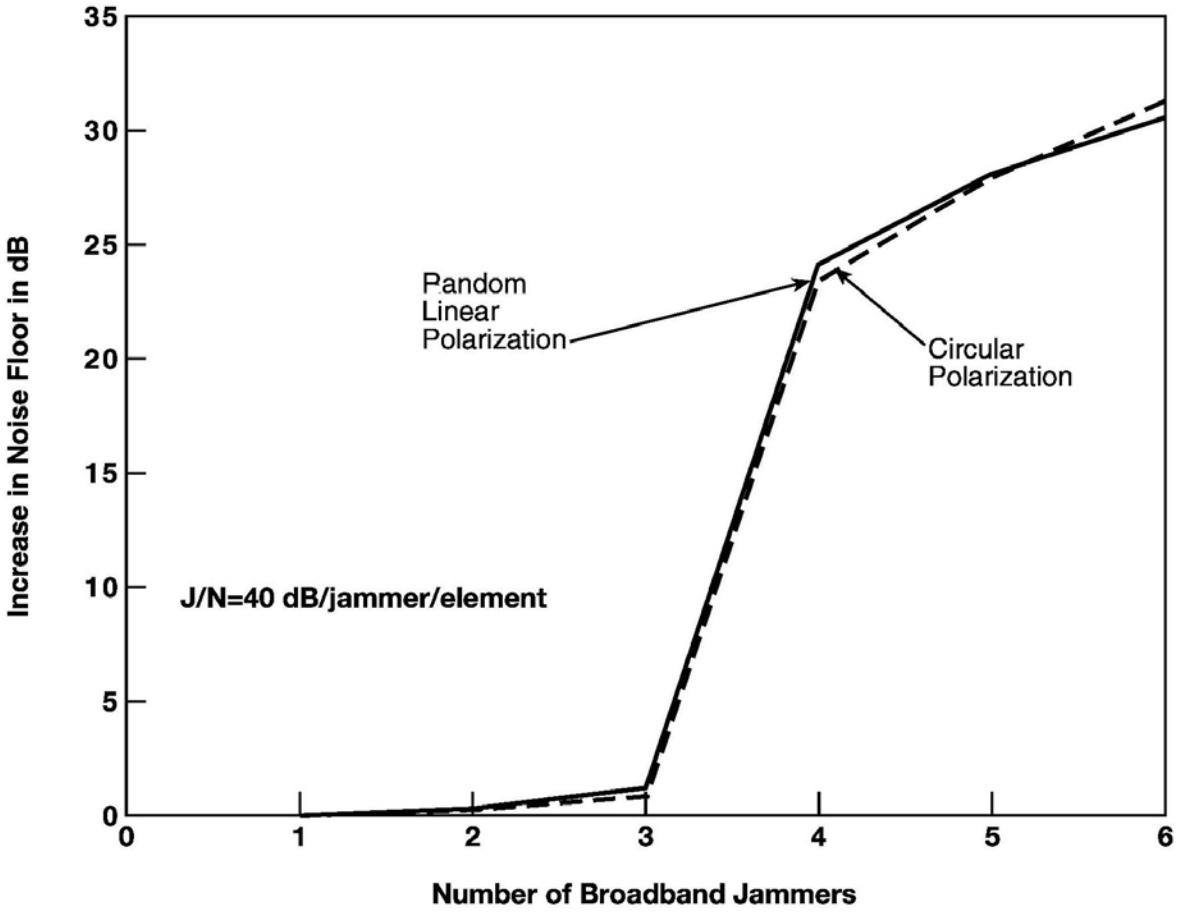

Figure 5. Performance of Two Dual-Polarized Antennas

It is interesting to note that the results for the interference-to-noise ratio after adaptation are relatively insensitive to the spacing between the dual-polarized element. That is, we obtain nearly the same (I + N)/N when the spacing d was equal to one quarter of a wavelength and one third of a wavelength as we did for one half wavelength. This is not true, however, for the signal-to-interference-plus-noise ratio, because closely spaced antennas produce a broader null on each jammer. This point is illustrated in Figure 6 where we show the single satellite availability for different separations d between the dual-polarized antennas. Note that as the separation decreases, the availability degrades.

The array with two dual-polarized antennas appears to be a potential possibility for a robust hand-held GPS receiver. In a non-dynamic environment State 5 lock can be maintained for C/N_o of only 18.5 dB-Hz and State 3 lock can be maintained for C/N_o of only 16 dB-Hz. Upon referring to Figure 6, we see that the probability of availability is nearly 0.95 even for separations as small as one-quarter wavelength, which at the L1 frequency (1.575 GHz) used by the GPS system is only about 2 inches. Thus, as long as mutual coupling doesn't lead to any significant problems, we can speculate that up to three broadband jammers can be cancelled using a

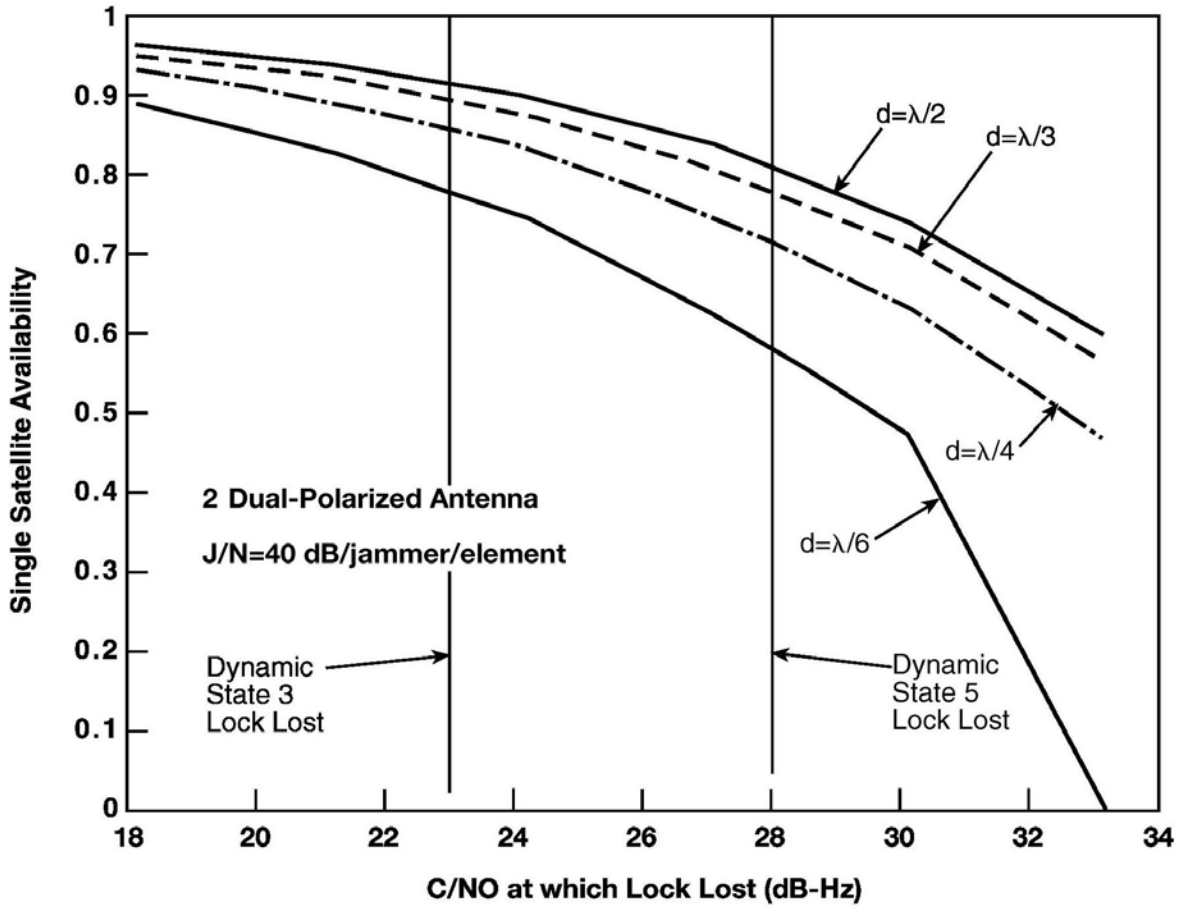

Figure 6. Availability in the Presence of Three Broadband Jammers

handheld GPS receiver (of course, the penalty is that each of the four elements must have its own receiver) with two dual-polarized antennas. Of course, two dual-polarized antennas are no better at cancelling three jammers than an array of four linearly-polarized antennas; they just occupy less real estate.

Next, let us consider four dual-polarized antennas (eight elements total). The dual-polarized antennas are located in the z = 0 plane (0,0), (0,d), (d,0), (d,d), where d is equal to one-half wavelength at midband. The increase in the noise floor (caused by the interferers) after adaptation versus the number of broadband jammers is shown in Figure 7. Each point is the average of 200 realizations of jammers with a random linear polarization located randomly in azimuth from 0° to 360° and randomly in elevation from 0° to 20° above the horizon. The results for the case when all jammers are circularly polarized were nearly identical, and thus not shown. Mutual coupling has again been ignored, and time taps were not employed.

When five adaptive time taps (K = 5) were placed behind each element, the increase in the noise floor in Figure 7 was reduced to nearly 0 dB for six jammers and to less than 1 dB for

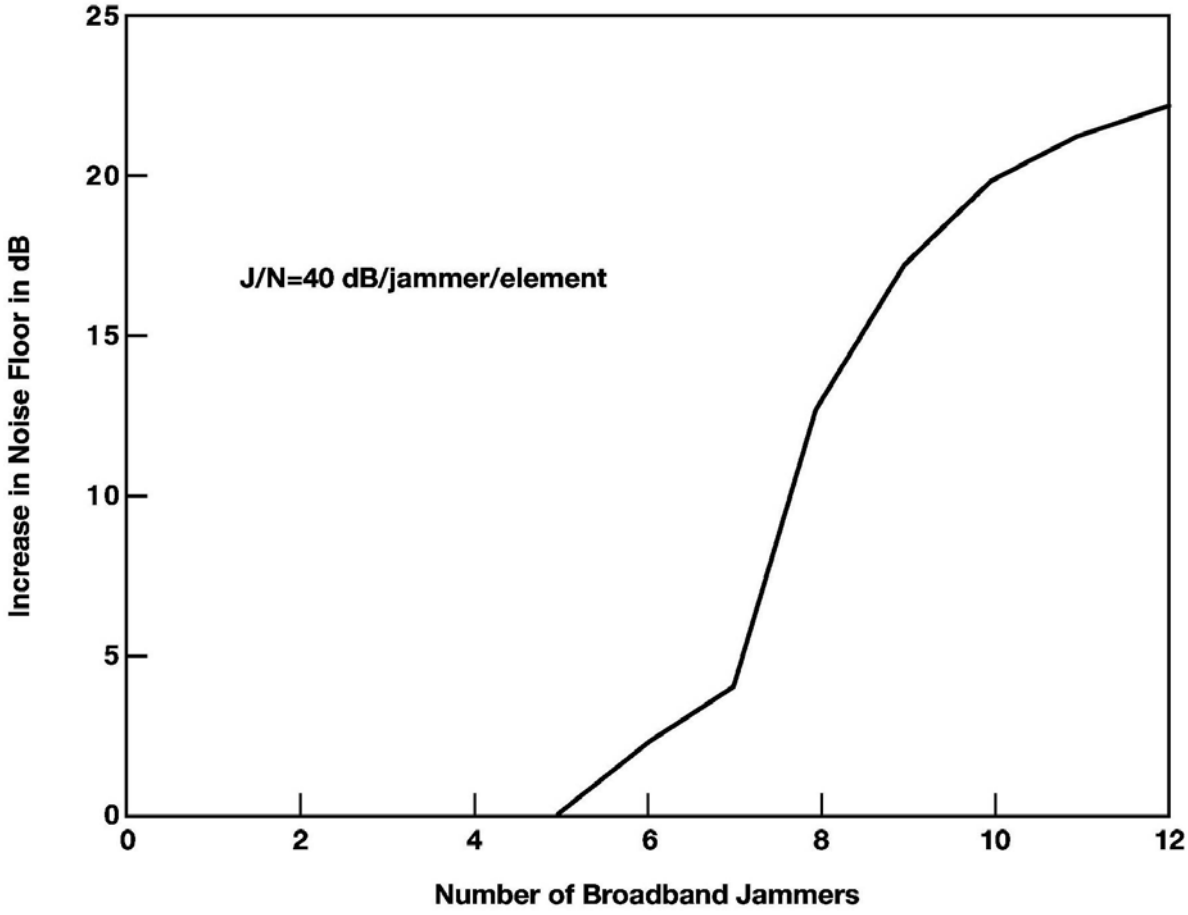

Figure 7. Performance of Four Dual-Polarized Antennas

seven broadband jammers, but for eight broadband jammers the increase in noise floor was again quite large. Thus, based on the results in Figures 3, 5, and 7, we conclude that an N-element, dual-polarized array can cancel N_J broadband interferers, where

$$N_J \simeq 2N - 1. \tag{32}$$

However, depending on interferer strength and system operating bandwidth, an adaptive filter with $K > 1$ time taps may be required behind each port in order to drive the interference below the noise floor.

The satellite availability for the array of four dual-polarized, square microstrip patch antennas is shown in Figure 8 for the cases of 1, 3, 5, and 7 broadband, randomly-located*

* That is, randomly located in azimuth in the elevation band 0° to 20° above the horizon.

interferers, each with a random linear polarization. We note that even when seven interferers are present, there is a significant probability of maintaining State 5 lock on a GPS satellite.

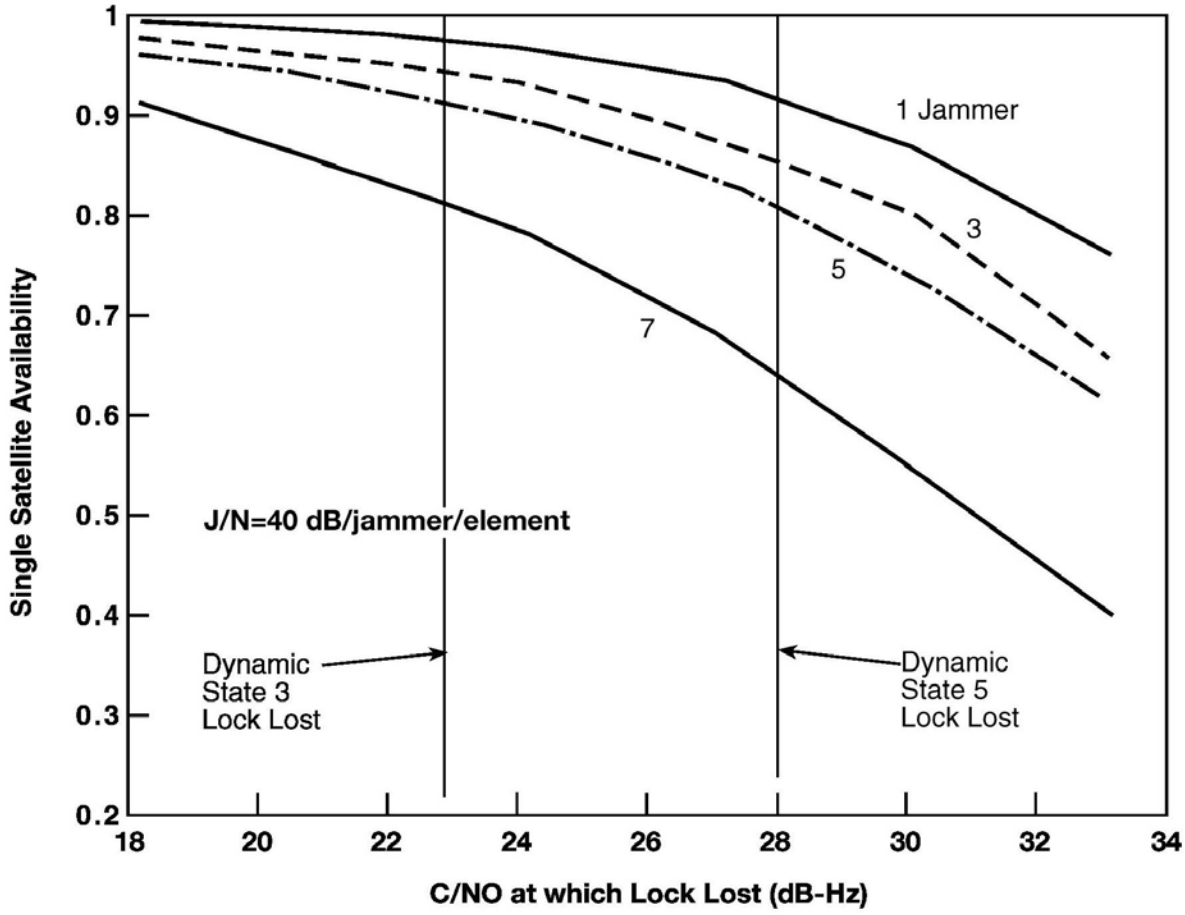

Figure 8. Availability for Four Dual-Polarized Antennas

It is interesting to estimate the effect of mutual coupling on array performance [20-21]. In order to do this we neglected the frequency dependence of the mutual coupling, and approximated the voltage coupling between the x-directed ports of different antennas by $0.2\exp(i\psi_{k\lambda})$, where $\psi_{k\lambda} = \text{random}\,(0,2\pi)$. This corresponds to –14 dB of coupling, which is slightly stronger than the values calculated in Reference 21. Similarly, for the voltage coupling between the y-directed ports of different antennas, we used $0.2\exp(i\gamma_{k\lambda})$, where $\gamma_{k\lambda} = \text{random}\,(0,2\pi)$. The voltage coupling between the x port of one antenna and the y port of another was approximated by $0.05\exp(i\tau_{k\lambda})$, where $\tau_{k\lambda} = \text{random}\,(0,2\pi)$. Finally, we ignored the coupling between the x and y ports of the same antenna.

The increase in the noise floor after adaptation for the array of four dual-polarized square, microstrip patches is shown in Figure 9. In order to stress the array, J/N has been increased to 50 dB/jammer/element. Each point is the average of 600 realizations of jammer locations, polarizations and mutual coupling coefficient phases (ψ,γ,τ). Based on this ultra simple model, it appears that mutual coupling has little effect on performance when the simple "power minimization" algorithm is used. We expect that its effect would be greater if we removed the assumptions that (a) the channel match is perfect (because then mismatch in one channel would be coupled into another channel) and (b) the coupling coefficients are independent of frequency across the operating band.

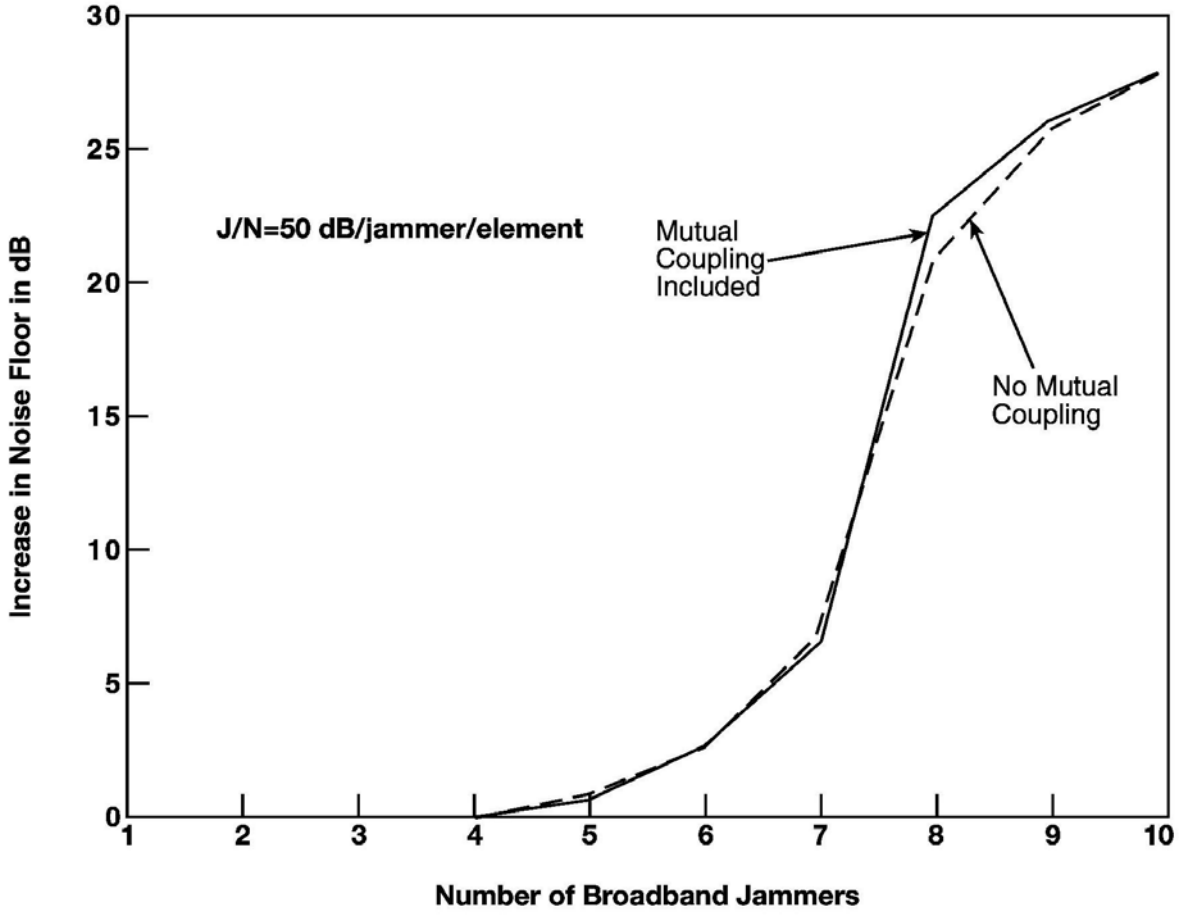

Figure 9. Performance of Four Dual-Polarized Antennas

VI. Discussion

We have demonstrated numerically that by combining dual-polarization with spatial and temporal degrees of freedom one can enhance the interference cancellation performance of an adaptive array without increasing its physical size. A single dual-polarized antennas was shown to cancel one randomly-located and randomly-polarized broadband jammer, but it fails against

two broadband jammers, even if both jammers have the same polarization state (e.g., both circularly polarized) but different locations. However, two dual polarized antennas separated (center-to-center) by at least one quarter of a wavelength easily cancelled three, randomly-located, broadband jammers near the horizon while simultaneously preserving the desired GPS signal space.

We then generalized the results to conclude that N dual-polarized antennas can cancel approximately 2N-1 broadband interferers. This result holds for arbitrary jammer polarization (linear, circular, elliptical), but does not hold for interferers that radiate independent, broadband noise on two orthogonal polarizations.

There is one set of published [22] data that clearly verifies the theoretical performance predictions for the space-time-polarization canceller. A square array of four microstrip patches has been constructed, with the center-to-center spacing between patches equal to one half wavelength. In this array, the two ports of the first element were connected so as to give a single circularly-polarized port, but the other three elements each had two orthogonal (i.e., x and y) linearly polarized ports. Thus, in this case, there are 6 degrees of freedom. Jammers (J/N = 45 dB) were then synthetically placed between –10° to +30° in elevation and from –170° to +170° in azimuth, and the null depth calculated. Null depth was defined as the ratio of the output power of the array to the input. In Figure 10, we compare the results presented in Reference 22 with our calculations obtained using the methods described in Sections 3 and 4. Observe the excellent agreement, and that even with six jammers present, the effective null depth is more than 30 dB.

Although in this paper we presented the analysis for the space-time-polarization (STP) canceller, a space-frequency-polarization (SFP) canceller works equally as well. In the SFP canceller there is a Q point FFT (fast Fourier transform) behind each antenna port that bins the received voltages into Q frequency bins. The interference is then cancelled [19, 23] independently in each frequency bin. We have studied the relative processing efficiencies of both of these approaches, and the conclusion has been that in some situations STP is better and in others SFP is better.

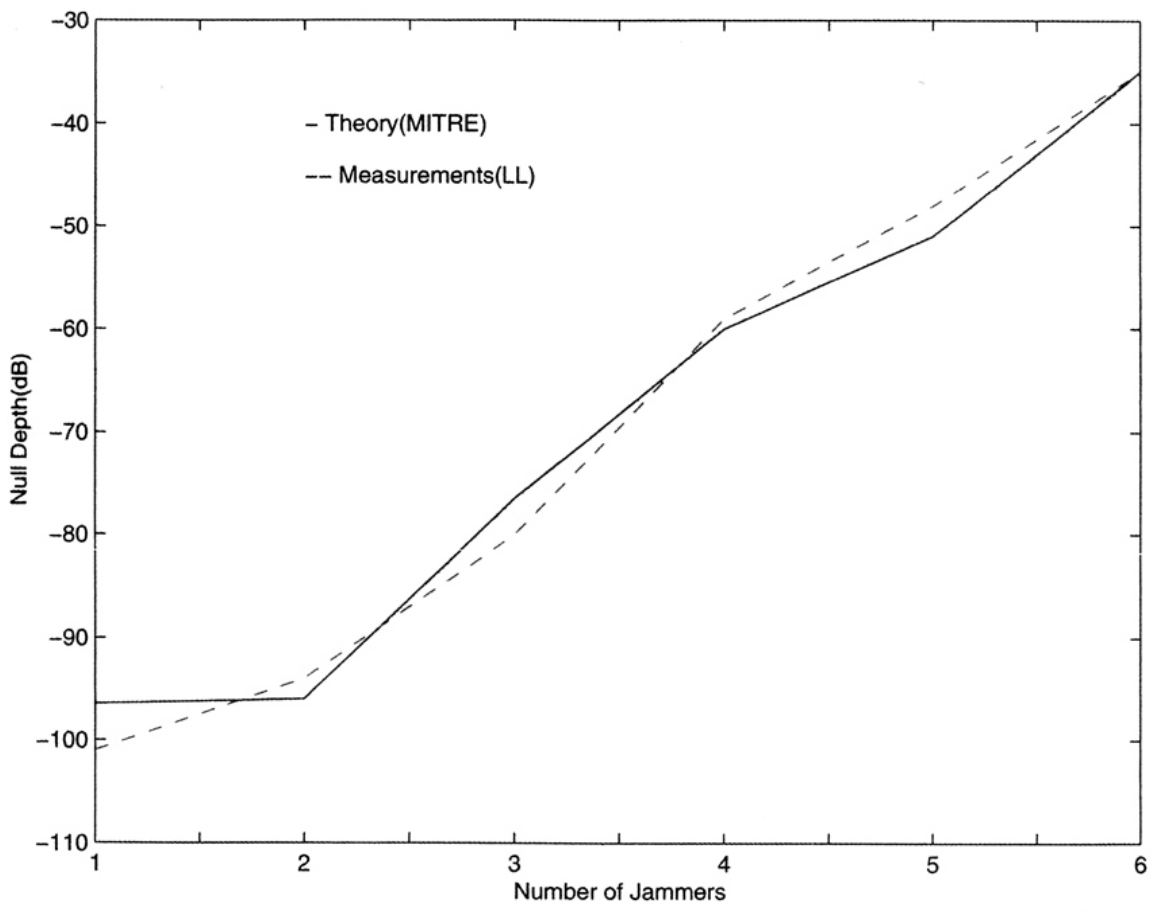

Figure 10. Comparison of Theoretical Null Depth Predictions with Reference 22

Acknowledgment

The author is grateful to John J. Vaccaro for multiple illuminating discussions on this topic.

List of References

1. A. J. Paulraj and C. B. Papadias, "Space-Time Processing for Wireless Communications," IEEE Signal Processing Magazine, November 1997, 49-83.

2. R. Monzingo and T. Miller, Introduction to Adaptive Arrays. New York, Wiley, 1980.

3. J. Ward, "Space-Time Adaptive Processing for Airborne Radar," Technical Report 1015, MIT Lincoln Laboratory, December 1994.

4. R. Compton, Adaptive Antennas. Englewood Cliffs, New Jersey, Prentice Hall, 1988.

5. J. Hudson, Adaptive Array Principles. London, Peter Peregrinus, 1989.

6. B. VanVeen, "Minimum Variance Beamforming," in S. Haykin and A. Steinhardt (Eds.), Adaptive Radar Detection and Estimation, New York, Wiley, 1992.

7. L. Brennan and I. Reed, "Theory of Adaptive Radar," *IEEE Transactions on Aerospace and Electronic Systems*, AES-9 (1973), 237-252.

8. A. Farina, Antenna-Based Signal Processing Techniques for Radar Systems. Boston, Artech House, 1992.

9. R. L. Fante and J. Vaccaro, "Wideband Cancellation of Interference in a GPS Receive Array," *IEEE Trans*. AES-36, pp. 549-564, April 2000.

10. O. Frost, "An Algorithm for Linearly-Constrained Adaptive Array Processing," *Proc. IEEE*, Vol. 60, pp. 926-935, 1972.

11. B. Widrow and S. Stearns, Adaptive Signal Processing. Prentice-Hall, 1985.

12. S. Applebaum, "Adaptive Arrays," *IEEE Trans*. AP-24, pp. 585-598, 1976.

13. P. Clarkson, Optimal and Adaptive Signal Processing. CRC Press, 1993.

14. L. Griffiths, "A Simple Adaptive Algorithm for Real-Time Processing in Adaptive Arrays," *Proc. IEEE*, Vol. 57, pp. 1696-1704, 1969.

15. J. Guerci, Space Time Adaptive Processing for Radar. Boston, Artech House, 2003.

16. E. Kaplan (Ed.), Understanding GPS: Principles and Applications. Boston, Artech House, 1996.

17. B. Parkinson and J. Spilker (Eds.), Global Positioning System: Theory and Applications. Washington, DC, American Institute of Aeronautics and Astronautics, 1996.

18. J. James, et al., Microstrip Antenna Theory and Design. P. Peregrinus, Ltd., pp. 77-80, 1989.

19. R. Fante and J. Vaccaro, "Ensuring GPS Availability in an Interference Environment," Proc. IEEE 2000 Precision Location and Navigation Symposium, pp. 37-40,2000 (ISBN: 0-7803-5872-4, IEEE Cat. No. 00CH37062).

20. I. Gupta and A. Ksienski, “Effect of Mutual Coupling on the Performance of Adaptive Arrays,” *IEEE Transactions on Antennas and Propagation*, 31 (1983), 785-791.

21. E. Ngsi and D. Blejer, “Mutual Coupling Analyses for Small GPS Adaptive Arrays,” IEEE SP-S International Symposium, Vol. 4, pp. 38-41, 2001.

22. E. Ngai, D. Blejer, T. Phuong, and J. Herd, “Anti-Jam Performance of Small GPS Polarimetric Arrays,” IEEE AP-S International Symposium, pp. 128-131, 2002.

23. I. Gupta, private communication at the Ohio State University, 1999.